Silicon (2020) 12:2301–2308
https://doi.org/10.1007/s12633-019-00325-z

ORIGINAL PAPER

Label Free Detection of Biomolecules Using SiGe Sourced Dual Electrode Doping-Less Dielectrically Modulated Tunnel FET

Amrita Singh[1] · S. Intekhab Amin[2] · Sunny Anand[1]

Received: 7 September 2019 / Accepted: 7 November 2019 / Published online: 3 January 2020

Abstract
In this work, the performance of a $Si_{0.5}Ge_{0.5}$ sourced dual electrode doping-less Tunnel FET (DEDLTFET) biosensor using dielectric modulation is studied for different cavity length, thickness (T_{bio}) and charge densities (QF). The use of silicon-germanium (SiGe) based source also shows an improvement in the performance of the charge plasma Tunnel FET because of its enhanced drain current. Biomolecules are introduced inside the cavity region and their impact on the drain current has been investigated to design the biosensor. The sensitivity factor of the biosensor depends upon the drain current obtained which is proportional to the dielectric constant (k) and the charge density of the biomolecules. The proposed biosensor achieves a maximum drain current sensitivity of 7.7×10^8 at a cavity length of 25 nm and 2.7×10^9 at a cavity length of 30 nm. When compared with the conventional TFET biosensors, it is observed that $Si_{0.5}Ge_{0.5}$ sourced doping-less TFET biosensor provides better drain current sensitivity.

Keywords Band-to-band tunneling (BTBT) · Dielectric modulation · Charge plasma · Biosensor · SiGe sourced TFET · Biomolecule sensitivity

1 Introduction

Nowadays, biosensors have a number of applications in the fields of medicine [1], agriculture and environment. FET based biosensors were first considered due to their low cost, on-chip integration and their compatibility with a wide range of biomolecules [2, 3]. However, a disadvantage of the FET based biosensors was their inability to detect neutrally charged biomolecules. For further improvement in performance, dielectrically modulated FETs were studied for detecting both charged and non-charged biomolecules [4]. Biomolecules were introduced underneath the gate through a cavity which was formed inside the insulator region [5]. It leads to the immobilization of biomolecules and the resultant effects were determined on the basis of the dielectric constant (k) and charge density of biomolecules. Furthermore, MOSFETs were introduced into the biosensing field. Unlike FETs, they poses the ability to detect the charged, non-charged as well as neutrally charged biomolecules [6, 7]. MOSFET based biosensors provide better performance because they result in higher drain current. However, in need to achieve a nanoscale device, the continuous scaling down of the channel length has led to short channel effects which has degraded the performance of the device. Also, it has limited the value of the subthreshold slope to a maximum of 60 mV/dec [8, 9].

Presently, Tunnel field effect transistors (TFETs) have become a promising device because of their ability of label free detection of biomolecules [10]. They are considered as the best possible alternative to MOSFETs because they achieve a lower subthreshold slope than 60 mV/dec and a lower leakage current. In a TFET, the flow of currents is based on Band-to-Band tunneling [11] which results in a desirable drain current which enhances the drain current sensitivity factor of the biosensor. Dielectrically modulated TFETs are even more efficient in achieving surpassing outcomes for drain current

✉ Sunny Anand
sunnyanand.42@gmail.com

Amrita Singh
singhamrita221@gmail.com

S. Intekhab Amin
intekhabamin@gmail.com

[1] Department of Electronics and Communication Engineering, Amity University, Sector-125, Noida, Uttar Pradesh 201313, India

[2] Department of Electronics and Communication Engineering, Jamia Millia Islamia, Jamia Nagar, New Delhi 110025, India

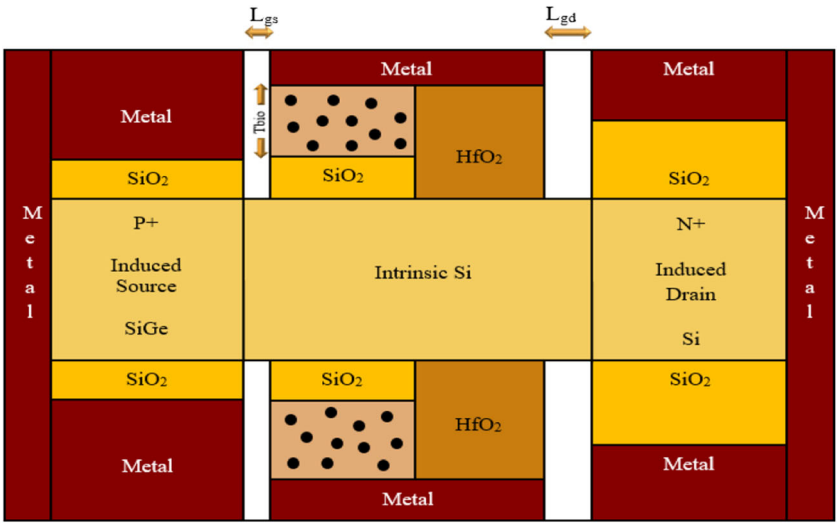

Fig. 1 2D structure of SiGe sourced DEDLTFET biosensor

sensitivity in comparison to the conventional TFET based biosensor. Inspite of achieving a lower subthreshold slope value, TFETs result in lower drain current values as compared to MOSFETs. Several techniques have been adopted to overcome this issue such as using a high-k gate dielectric material [12], gate stacking [13], dual material gate [14], etc. Beside these techniques, the use of a low bandgap material, SiGe, also enhances the drain current. As a result of the wide energy band gap of silicon, the conventional silicon sourced TFETs have lesser drain current than MOSFETs. The drain current of the TFETs can be improved by increasing the probability of tunneling on the source side. Hence, the low bandgap material is used at the source side to achieve a high drain current value while a high band gap material is used at the drain side to obtain a low leakage current value.

Achieving uniform doping in nanoscale devices is challenging [14]. TFET requires abrupt source-channel and drain-channel junctions which can be developed by applying the charge plasma technique [15]. In this technique, source and drain regions are created in the silicon substrate by using metals of suitable work functions.

We have proposed a SiGe sourced DEDLTFET [16, 17] based biosensor. The sensitivity of a biosensor is proportional to its drain current value. Higher the value of drain current, better will be the drain current sensitivity. Biosensors detect the biological elements by converting the biological response into electrical signals. Cavities are introduced towards the source side under the metal gate to allow the entry of biomolecules which are introduced in terms of dielectric constants (k) [5]. The presence of biomolecules, either positive or negative, modulates the electrical parameters of the device which result in the detection of biomolecules. The double gate metals helps in providing better control of the device [18]. The high-k material used as insulator between gate and substrate will improve the drain current because the value of drain current is proportional to the dielectric constant. Therefore, HfO_2, a high-k material has been used as the dielectric [12].

This paper focuses on label free sensing [10, 19] by investigating the response of different biomolecules on the performance of the device. The outcomes for different cavity lengths

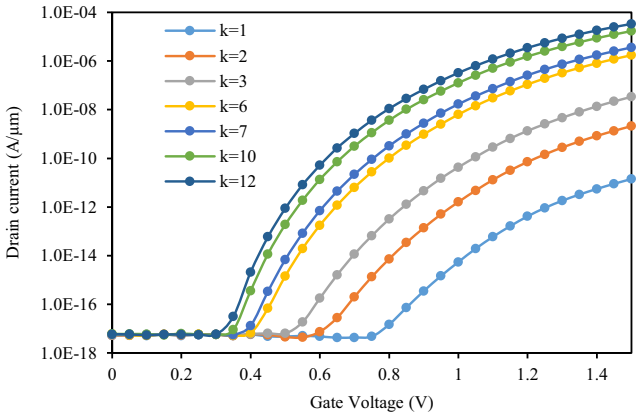

Fig. 2 Transfer characteristics of SiGe sourced DEDLTFET with different values of dielectric constant (k) for cavity length 25 nm

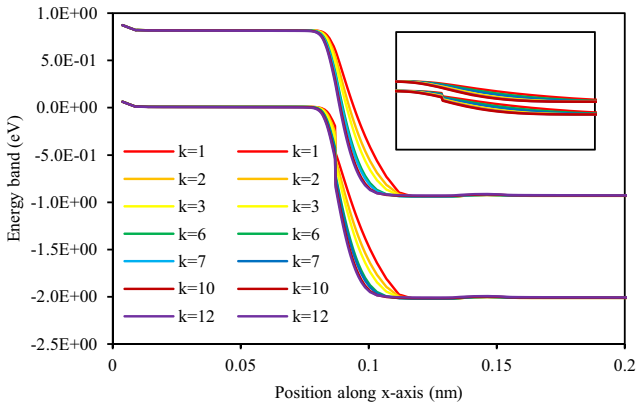

Fig. 3 Energy band diagram for SiGe sourced DEDLTFET with different values of dielectric constant (k) for cavity length 25 nm

and thicknesses are observed. The impact of different charge densities, both positive and negative, has also been studied and discussed in the results section in detail.

2 Device Structure

The device specifications of SiGe sourced DEDLTFET biosensor are as follows: the thickness of the silicon substrate (T_{si}) is 10 nm, the channel length (L) is 50 nm and the gate oxide thickness (t_{ox}) is 5 nm and has an intrinsic carrier concentration (n_i) of 1×10^{15} atoms cm^{-3}. The source and the drain regions are developed by using suitable metal work functions on the source and drain sides for a charge plasma based TFET. The P^+ region at the source side is formed by introducing a platinum electrode (WF = 5.93 eV) while a hafnium electrode (WF = 3.9 eV) is used at the drain side to form the N^+ region. The germanium content in the SiGe compound is 50% which enables an acquisition of an energy band gap (Eg) of 0.94 eV. Whereas silicon has an energy band gap (Eg) of 1.12 eV which is greater than that of $Si_{0.5}Ge_{0.5}$. Cavities are formed underneath the gates afterwards and these, in turn, are introduced with different biomolecules to get the device electrically modulated to detect the biomolecules. Figure 1 shows the SiGe sourced DEDLTFET biosensor where the regions underneath the gate metals are divided into two sections. Cavity is introduced at the source side with its length varying between 25 and 30 nm and the gate oxide (HfO_2) is introduced at the drain side whose length varies between 20 and 25 nm. The work function of the metals over both the gates is 4.4 eV. The gap between the gate and source metal (L_{gs}) is kept as

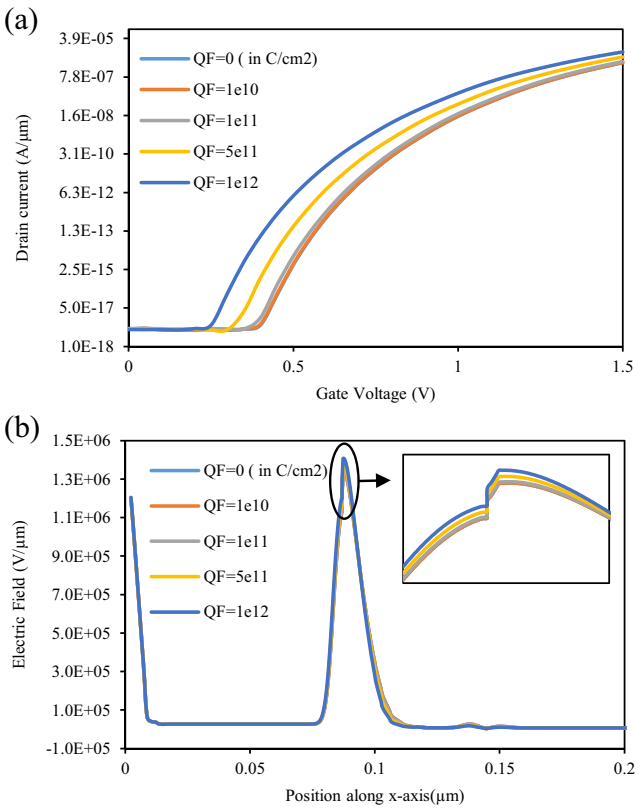

Fig. 4 **a** Drain Current and **b** Electric Field for SiGe sourced DEDLTFET with cavity length 25 nm and dielectric constant (k) = 7 for different positive charge densities

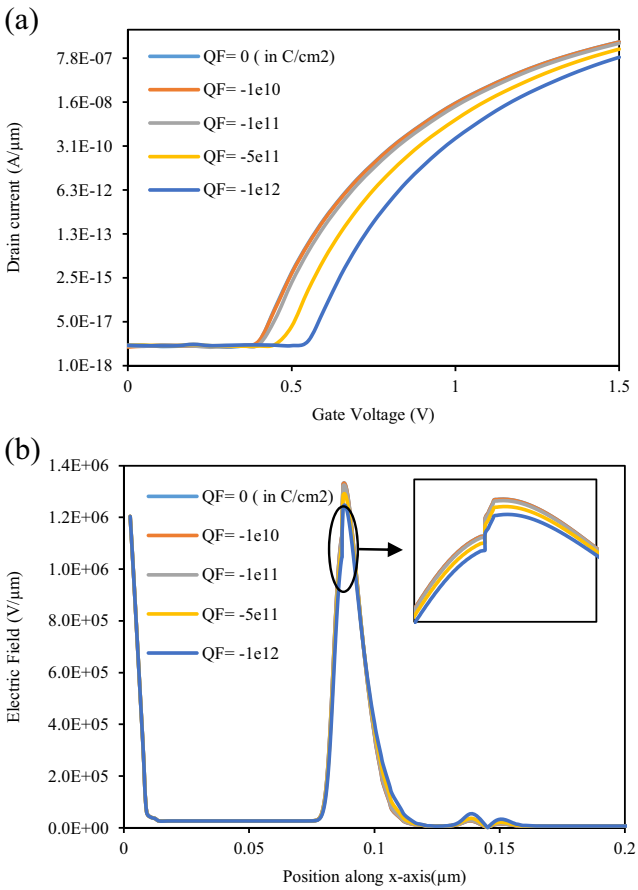

Fig. 5 **a** Drain Current and **b** Electric Field for SiGe sourced DEDLTFET with cavity length 25 nm and dielectric constant (k) = 7 for different negative charge densities

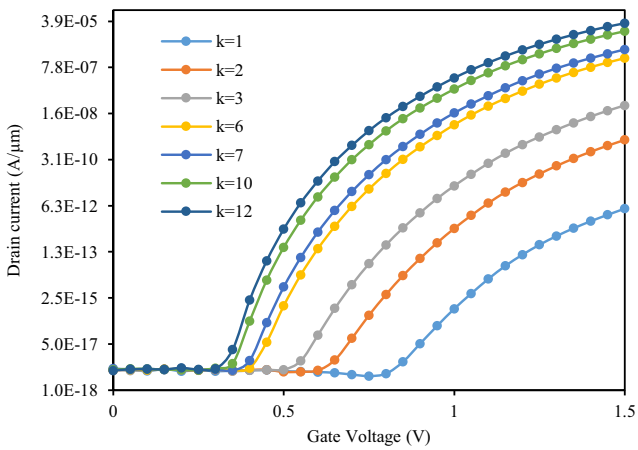

Fig. 6 Transfer characteristics of SiGe sourced DEDLTFET with different values of dielectric constant (k) for cavity length 30 nm

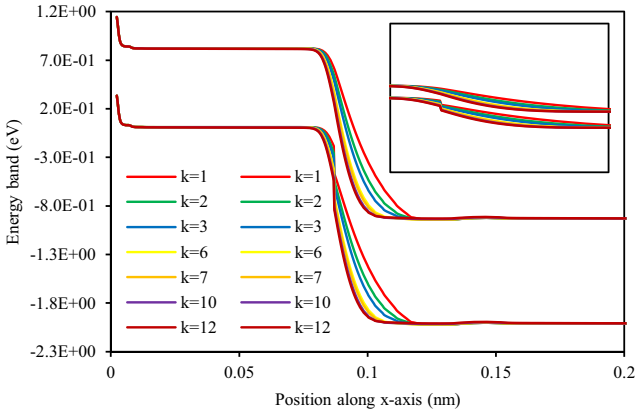

Fig. 7 Energy band diagram for SiGe sourced DEDLTFET with different values of dielectric constant (k) for cavity length 30 nm

3 nm and between gate and drain metal (L_{gd}) is taken to be as 15 nm [20]. As shown in Fig. 1, L_{gs} is lesser than L_{gd}. This has been designed as such because L_{gs} is the determining factor in the electron tunneling probability from source to channel. A 0.5 nm thick layer of silicon dioxide is introduced between the source electrode and the SiGe source to avoid the formation of silicide. Also, a 3 nm thick layer of silicon dioxide is introduced between the silicon substrate and drain electrode for the same reason [21].

The simulation results were achieved by using Silvaco TCAD Atlas tool [22]. In the simulations, drift- diffusion current transport model is proposed for the tunneling of electrons and holes. The concentration dependent Shockley-Read-Hall recombination, Lombardi mobility (CVT) model and generation model account for the effects of leakage current and the mobility of electrons. Non-local BTBT model is considered to account for the separation of holes generated in the valence band and electrons originated in the conduction band.

3 Results and Discussion

The drain current of DEDLTFET depends upon the Band-to-band tunneling of electrons from valence band of source to the conduction band of channel. Higher the tunneling probability, more will be the drain current. The low bandgap material $Si_{0.5}Ge_{0.5}$ used at the source side increases the probability of tunnelling T(E) that is given by Eq. 1.

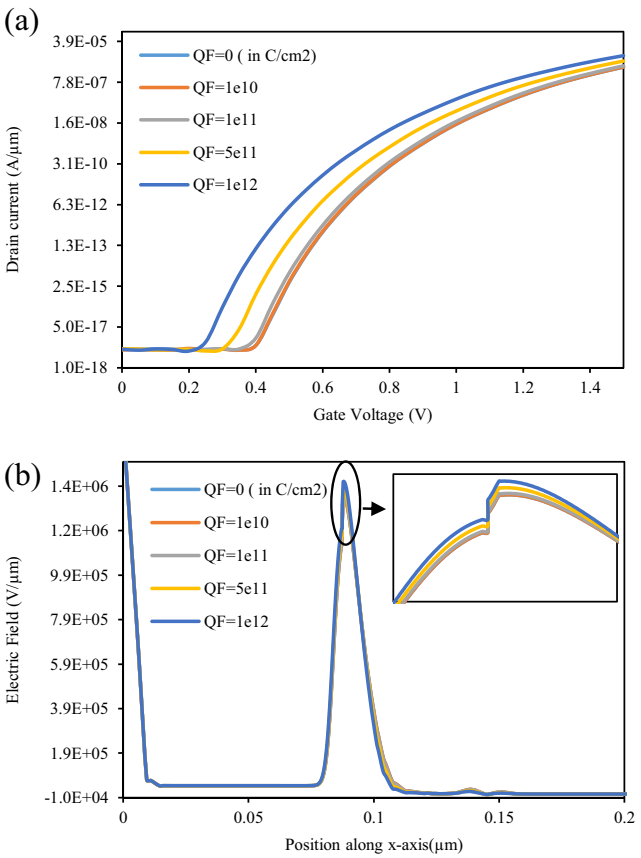

Fig. 8 **a** Drain Current and **b** Electric Field for SiGe sourced DEDLTFET with cavity length 30 nm and dielectric constant (k) = 7 for different positive charge densities

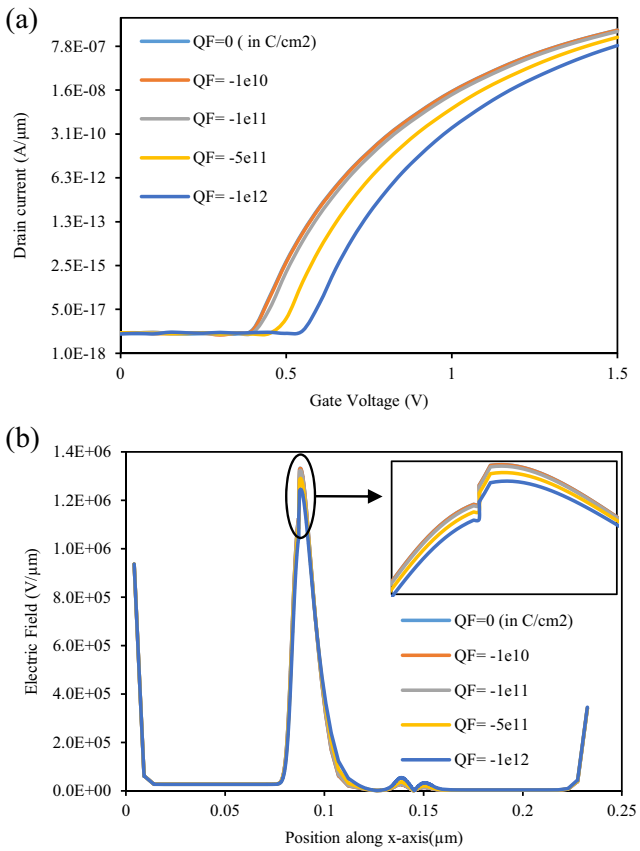

Fig. 9 **a** Drain Current and **b** Electric Field for SiGe sourced DEDLTFET with cavity length 30 nm and dielectric constant (k) = 7 for different negative charge densities

$$T(E) = \exp\left(\frac{-4\lambda\sqrt{2m}E_g^{\frac{3}{2}}}{3\,|e|h\left(E_g + \Delta\Phi\right)}\right)\Delta\Phi \quad (1)$$

$$\text{Screening length, } \lambda = \sqrt{\frac{\epsilon_{si}}{\epsilon_{ox}}t_{si}t_{ox}}$$

The tunneling probability is inversely proportional to the screening length (λ). It can be downsized by using a high-k gate oxide material or by lowering the thickness of the gate oxide. The role of biomolecules in the BTBT process is at the source-channel junction. The immobilization of the biomolecules accelerates the flow of electrons with different dielectric constants (k) and charge densities of biomolecules. The use of $Si_{0.5}Ge_{0.5}$ at source side improves the drain current and also lowers the value of the leakage current because of its low energy bandgap.

The lengths of the cavity are set as 25 nm and 30 nm during simulations. Figure 2 shows the I_D-V_{GS} characteristics during the immobilization of the biomolecules with different dielectric constants (k) for cavity length 25 nm at V_{DS} = 1.5 V. It is noticed that with an increase in the permittivity of the dielectric constant of the biomolecules, the drain current increases simultaneously. The cavity introduced under the gate increases the tunneling barrier which leads to a low probability of electron tunneling. The introduction of SiGe results in a lowered barrier between the valence band of the source and the conduction band of the channel. With an addition of the biomolecules with some dielectric constant, the barrier width reduces whereas the leakage current remains minimum as shown in Fig. 3. Therefore, there is a sudden increment in the drain current to leakage current ratio (I_{on}/I_{off}), thus improving the subthreshold slope that is given by Eq. 2.

$$S = \frac{V_t - V_{OFF}}{log\ I_{vt} - log\ I_{OFF}} \quad (2)$$

The detection of neutrally charged biomolecules is based on the dielectric constant while that of the charged ones is based on the dielectric constant (k) as well as on the charge density of the biomolecules. In Fig. 4(a), a biomolecule with different positive charge densities (QF) are immobilized. We know that $q = cv$ and the charge density is proportional to the current. An increase in the charge density increases the drain current because it reduces the band gap between the valence

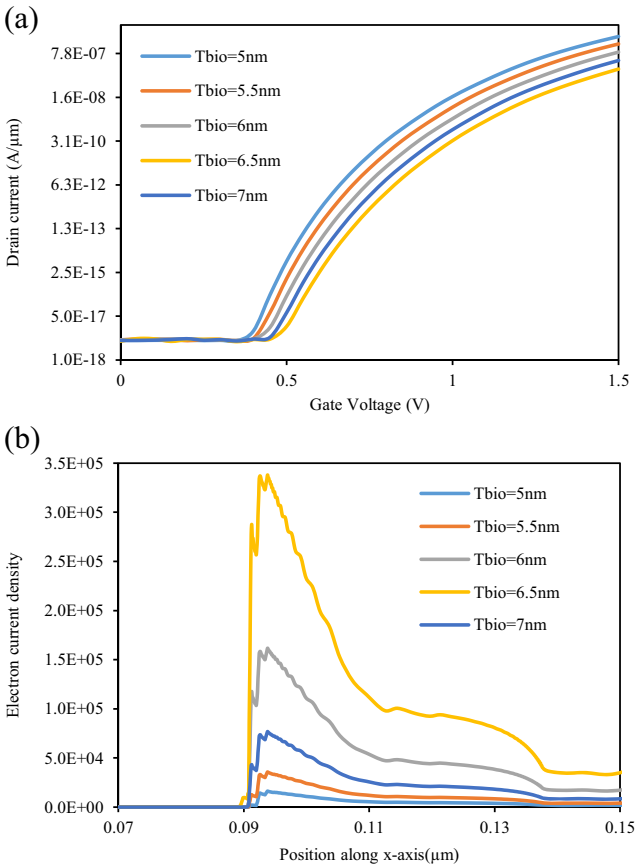

Fig. 10 **a** Drain Current and **b** Electron current density for SiGe sourced DEDLTFET with cavity length 30 nm and dielectric constant (k) = 7 for different cavity thickness

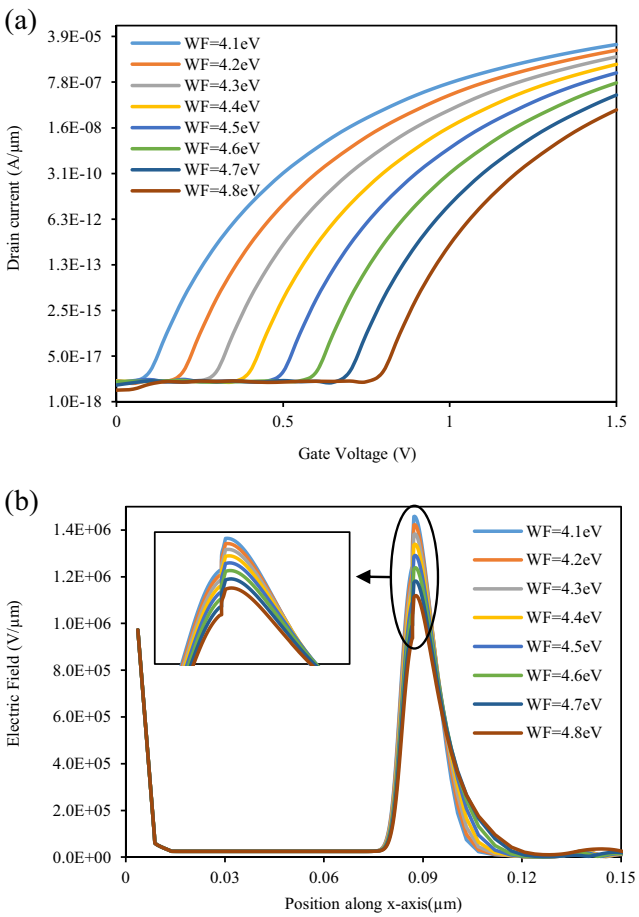

Fig. 11 **a** Drain Current and **b** Electric field for SiGe sourced DEDLTFET with cavity length 30 nm and dielectric constant (k) = 7 for different work functions

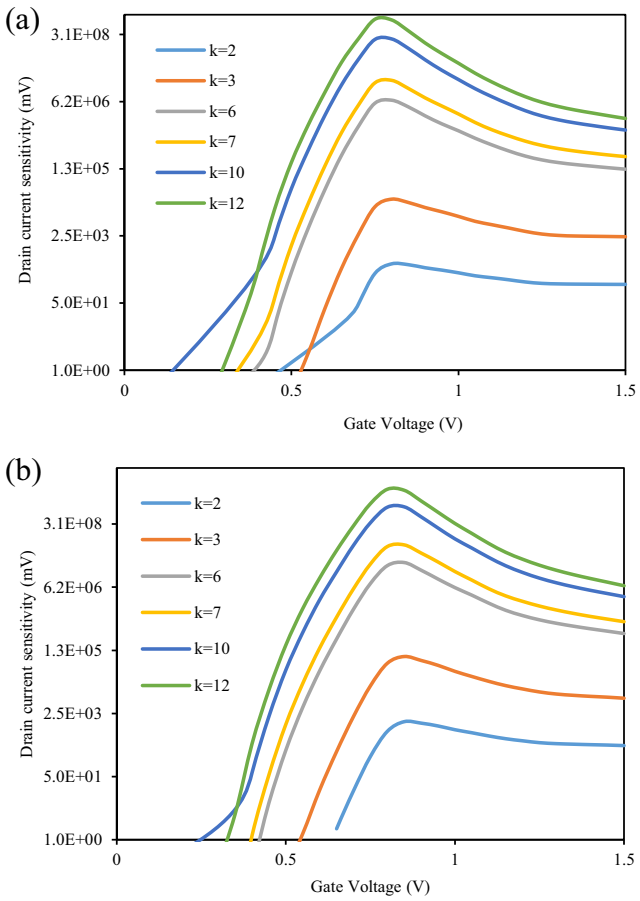

Fig. 12 Drain current sensitivity plots of SiGe sourced DEDLTFET for cavity length **a** 25 nm and **b** 30 nm

band of source and the conduction band of channel. It is observed that with an increase in the charge density, the drain current also increases. Figure 4(b) shows the electric field plot for the positive charge density. It justifies the increment in drain current as the value of the electric field increases. Electric field is inversely proportional to the cavity length which indicates an increase in the tunneling of electrons.

Figure 5(a) shows the negative charge densities with dielectric constant k = 7 that result in similar observations as discussed previously. Although the value of drain current is less as compared to the positive charge densities due to the low charge density, an increment in the charge densities leads to an increment in the drain current. Figure 5(b) shows the electric field produced by the negative charge densities. Similar to the positive charge densities, it justifies the raise in drain current value as the value of the charge densities increases. A high electric field value indicates an improvement in the tunneling of electrons which leads to a higher drain current value.

Figure 6 shows the I_D-V_{GS} characteristics during the immobilization of the biomolecules with different dielectric constants for cavity length of 30 nm at V_{DS} = 1.5 V. It is observed that because of an increment in the cavity length, there is a slight decrement in the drain current. It occurred as a result of an increase in the channel length that widened the energy bandgap which resulted in decreased tunneling of electrons. With an increase in the cavity length, the capacitance between the gate-channel region decreases because $C = \varepsilon A/l$. Thus, an increase in the cavity length affects the drain current. In Fig. 7, energy bands for biomolecules with different dielectric constants shows that the biomolecules with higher dielectric constants have lower bandgap. The introduction of $Si_{0.5}Ge_{0.5}$ contracts the band gap and with the addition of biomolecules, the band gap continues to lower which also results in greater electron tunneling.

In Fig. 8(a), a biomolecule with varying positive charge densities are immobilized for cavity of length 30 nm and having a dielectric constant of 7. As discussed earlier, it poses the same explanation as in the case of cavity length of 25 nm besides the slight decrement observed in the drain current value. Since, charge density is proportional to the current, an increase in the charge density promotes the drain current. Figure 8(b) depicts the electric field for the positive charge densities for cavity of length 30 nm. It explains the increment in the value of the drain current observed for the increment observed in the value of electric field.

Figure 9(a) shows the variation in drain current for a biomolecule with negative charge densities for a cavity length of 30 nm and dielectric constant 7. The value of the drain current obtained in this case is less as compared to that in the case of the positive charge densities due to a low charge density. However, the drain current still shows an improvement with

Table 1 Comparative analysis of different proposed devices

Reference	Year	Material	I_{on} (A/μm)	I_{on} /I_{off}	Sensitivity
Proposed work	–	SiGe Source	16.9 μ (k = 10)	2.77×10^{12}	2.43×10^{8}
Sing D et.at. [23]	2017	Si	0.12 μ (k = 10)	9.42×10^{9}	9.48×10^{5}
Noor SL et.at. [24]	2007	Si	6.44 μ (Aptes)	5.05×10^{11}	4.82×10^{7}
Shafi N et.at. [25]	2017	SiGe Source	0.05 μ (k = 5)	5.71×10^{7}	0.66×10^{3}

an increase in the value of charge densities. Figure 9(b) represents the electric field formed by the negative charge densities. Similar to the previous discussions, it explains the raise in the drain current value which is proportional to the increasing charge densities. Higher value of electric field implies better tunneling of electrons which leads to better results.

Figure 10(a) represents the outcomes of varying the cavity thickness (T_{bio}) on drain current. It is observed that with an increase in the cavity thickness, there is a drop in the drain current. It happens because increasing the cavity thickness results in a wider tunneling barrier at the source-channel interface, which lowers the probability of tunneling. It is also noticed that for a cavity thickness of 5 nm, drain current achieves its maximum value. Figure 10(b) shows the electron current density obtained when tunneling of electrons at different cavity thicknesses takes place.

In Fig. 11(a), drain current is observed for different metal work function (WF) values when the dielectric constant and the cavity length have been fixed. The work function of the metal is inversely proportional to the drain current. As the work function increases, the concentration of holes rises and the flow of electrons reduces which results in the lowering of drain current value. The values of electric field with respect to different work functions is shown in Fig. 11(b). It is clear that more electric field is induced within the device as the tunneling barrier becomes smaller. Also, with an increase in the metal work function, the electric field declines proportionally.

Drain current sensitivity is detected by analyzing the difference between drain current induced by the immobilized biomolecules (I_d (bio)) with respect to drain current induced by air (I_d (air)) in a biosensor as shown in Eq. 3 [21, 23, 24].

$$Sensitivity = \frac{I_d(bio) - I_d(air)}{I_d(air)} \quad (3)$$

Figure 12 shows the relevant drain current sensitivity plots for different cavity lengths for varying dielectric constants. In Fig. 12(a), the sensitivity plot for the cavity length of 25 nm is shown and Fig. 12(b) shows the sensitivity plot for the cavity length of 30 nm. With an increase in the dielectric constant, the drain current increases which simultaneously, also, results in an increment in the drain current sensitivity of the device. Whenever there is a moderate change in the dielectric constant, the drain current sensitivity factor is observed to have been escalated. The introduction of SiGe in the source region of the DEDLTFET provides better drain current than the conventional DEDLTFET. Higher the drain current, more will be the drain current sensitivity of the device.

A comparative analysis of the proposed device with other biosensor devices has been done and given in Table 1. It is observed that the SiGe sourced DEDLTFET provides better drain current (I_{on}) value and the I_{on}/I_{off} ratio is also significantly higher. The maximum sensitivity attained by the proposed devices has also been compared.

4 Conclusion

In this paper, we observed that $Si_{0.5}Ge_{0.5}$ sourced DEDLTFET provides a superior performance in terms of drain current than Si based DEDLTFET for both cavity lengths - 25 nm and 30 nm. The immobilization of biomolecules following the incorporation of $Si_{0.5}Ge_{0.5}$ at the source side offers several advantages in terms of drain current sensitivity of the device. Based on the results, it is observed that the biosensor with cavity lengths 25 nm and 30 nm has a very little difference in the calculated parameters. Since 25 nm cavity length provides marginally higher drain current, it is proposed to be more beneficial. Biosensors are highly dependent on the sensitivity factor. Higher the drain current, higher will be the drain current sensitivity. The $Si_{0.5}Ge_{0.5}$ sourced DEDLTFET with cavity length 25 nm acquires the ability to meet the requirements of an efficient biosensor. Thus, taking the different cavity lengths, their thicknesses (T_{bio}), charge densities (QF) and dielectric constants (k) into consideration, it can be concluded that $Si_{0.5}Ge_{0.5}$ sourced DEDLTFET based biosensor exhibits a better performance as compared to the Si based DEDLTFET biosensor. Moreover, the leakage current of the proposed device remains at its minimum throughout, thus making it more desirable.

References

1. Bergveld P (1986) The development and application of FET-based biosensors. Biosensors 2(1):15–33
2. Sarkar D, Banerjee K (2012) Proposal for tunnel-field-effect-transistor as ultra-sensitive and label-free biosensors. Appl Phys Lett 100(14):143108
3. Amin SI, Gajal L, Anand S (2018) Analysis of dielectrically modulated doping-less transistor for biomolecule detection using the charge plasma technique. Appl Phys A Mater Sci Process 124(9): 578
4. Collaert N, Voon Yew T (2019) "FET biosensor." U.S. Patent Application 10/309,925, filed June 4
5. Gu B, Park TJ, Ahn J-H, Huang X-J, Lee SY, Choi Y-K (2009) Nanogap field-effect transistor biosensors for electrical detection of avian influenza. Small 5(21):2407–2412
6. Shreya S, Khan AH, Kumar N, Amin I, and Anand S, "Core-Shell Junctionless nanotube tunnel field effect transistor: design and sensitivity analysis for biosensing application", IEEE Sensors J, https://doi.org/10.1109/JSEN.2019.2944885
7. Narang R, Saxena M, Gupta M (2015) Investigation of dielectric modulated (DM) double gate (DG) junctionless MOSFETs for application as a biosensors. Superlattice Microst 85:557–572
8. Bentrcia, T, Djeffal F, Ferhati H, and Dibi Z (2019) "A Comparative Study on Scaling Capabilities of Si and SiGe Nanoscale Double Gate Tunneling FETs." Silicon pp.1–9

9. Bala S, Khosla M (2018) Design and simulation of nanoscale double-gate TFET/tunnel CNTFET. J Semicond 39(4):044001
10. Anand S, Singh A, Amin SI, and Thool A (2019) "Design and Performance Analysis of Dielectrically Modulated Doping-less Tunnel FET based Label Free Biosensor." IEEE Sensors J
11. Tsai T-C, Lin C-T, Wang L-T, Peng C-T, Chen D-F, Lin H-T, and Wang C-H (2018) "Tunnel field-effect transistor." U.S. Patent 9, 941,394, issued April 10
12. Boucart K, Ionescu AM (2007) Length scaling of the double gate tunnel FET with a high-k gate dielectric. Solid State Electron 51(11–12):1500–1507
13. Wu C, Huang Q, Yang Z, Wang J, Wang Y, Huang R (2016) A novel tunnel FET design with stacked source configuration for average subthreshold swing reduction. IEEE Trans Electron Dev 63(12):5072–5076
14. Obite F, Ijeomah G, Bassi JS (2019) Carbon nanotube field effect transistors: toward future nanoscale electronics. Int J Comput Appl 41(2):49–164
15. Anand S, Amin SI, Sarin RK (2016) Performance analysis of charge plasma based dual electrode tunnel FET. J Semicond 37(5):054003
16. Singh G, Amin SI, Anand S, Sarin RK (2016) Design of Si0. 5Ge0. 5 based tunnel field effect transistor and its performance evaluation. Superlattice Microst 92:143–156
17. Anand S, Sarin RK (2016) Analog and RF performance of doping-less tunnel FETs with $$\hbox {Si} _ {0.55}\hbox {Ge} _ {0.45} $$ Si0. 55Ge0. 45 source. J Comput Electron 15(3):850–856
18. Anand S, Intekhab Amin S, Sarin RK (2016) Analog performance investigation of dual electrode based doping-less tunnel FET. J Comput Electron 15(1):94–103
19. Narang R, Sasidhar Reddy KV, Manoj S, Gupta RS, Gupta M (2012) A dielectric-modulated tunnel-FET-based biosensor for label-free detection: analytical modeling study and sensitivity analysis. IEEE Trans Electron Dev 59(10):2809–2817
20. Anand S, Sarin RK (2016) An analysis on Ambipolar reduction techniques for charge plasma based tunnel field effect transistors. J Nanoelectron Optoelectron 11(4):543–550
21. Kumar MJ, Janardhanan S (2013) Doping-less tunnel field effect transistor: design and investigation. IEEE Trans Electron Dev 60(10):3285–3290
22. ATLAS (2012) Device simulation software. Silvaco Int, Santa Clara
23. Singh D, Pandey S, Nigam K, Sharma D, Yadav DS, Kondekar P (2017) A charge-plasma-based dielectric-modulated junctionless TFET for biosensor label-free detection. IEEE Trans Electron Dev 64(1):271–278
24. Noor SL, Khan MZ (2017) "Application of nanocavity embedded dual metal double gate TFET in biomolecule detection," In Humanitarian Technology Conference (R10-HTC) IEEE Region, pp. 345–348
25. Shafi N, Sahu C, Periasamy C, Singh J (2017) SiGe source charge plasma TFET for biosensing applications. In Nanoelectronic and Information Systems (iNIS), 2017 IEEE International Symposium, pp. 93–98